

# Clogging of soft particles in 2D hoppers

Xia Hong, Meghan Kohne, and Eric R. Weeks

*Department of Physics, Emory University, Atlanta, GA 30322, USA*

(Dated: August 16, 2016)

We experimentally study the flow of oil-in-water emulsion droplets through a quasi-two-dimensional hopper. The hopper chamber is sufficiently thin so that the droplets are deformed into pancake shapes. Due to surfactants coating the droplets, they easily slide past each other, approximating soft frictionless disks. We find that clogging at the hopper exit requires a narrow hopper opening only slightly larger than the droplet diameter. This is in contrast to previous studies with hard disks that found arch formation and clogging with significantly larger hopper openings. We conduct simulations demonstrating that softness is the key factor reducing clogging for emulsion droplets. With stiffer droplets or a stronger gravitational force, clogging is easier.

PACS numbers: 47.57.Bc, 83.80.Iz, 45.70.Mg

## I. INTRODUCTION

Flowing sand differs qualitatively from flowing fluid and understanding the differences leads to interesting physics [1, 2]. A dramatic difference is seen in the gravity-driven flow of sand out of a hopper: when the exit opening from a hopper is small, the sand can clog at the hopper exit [3, 4]. The existence of a critical exit opening size of 3-6 particle diameters has been long known [5–11]. Even when the hopper opening is slightly larger, and clogs do not form, the flow is influenced by the possibility of clogging: for example, there are fluctuations of the flow rate of the sand [3, 12–14]. The mean flow rate is a function of the difference of the opening size to the critical size for clogging, a result often attributed to Beverloo [7] although mentioned by earlier authors as well [5]; see a discussion of the history in Ref. [8]. In this sense, understanding what happens when hoppers clog – and the size of the opening that causes clogging – is crucial for understanding the flow properties when the opening is larger than the critical size [4, 7, 8]. We note that some experiments suggest that clogging does not have a critical size but rather becomes exponentially unlikely as the hopper opening increases [15–17]; nonetheless, it's clear that understanding the flow properties requires understanding the clogging probability.

The clogging process itself is due to arch formation at the hopper exit [13, 16, 18]. The difficulty of forming large arches is the reason why hoppers do not clog when their exit opening is sufficiently large [18]. Friction may be important for the formation of these arches [18], and more generally it has long been seen that friction influences hopper flow to an extent [5, 8, 12, 14, 19]. However, it was unclear exactly how friction played a role – friction influences the angle of repose [19] and the packing density [7], for example, but it was unclear which of these (if either) influences the flow rate or clogging. A different experiment studied the flow of foams, and showed that the softness of the bubbles influenced the flow [20]. In this case, there was no static friction. Due to the ability of bubbles to deform, clogging required the exit orifice to be smaller than the mean bubble size, and this pro-

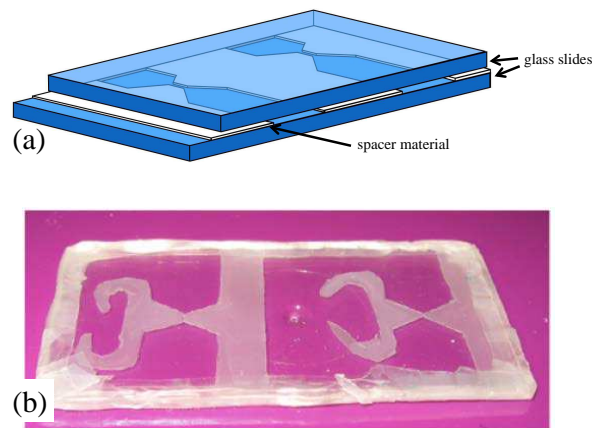


FIG. 1: (a) Sketch of sample chamber construction. (b) Photograph of a typical sample chamber constructed from parafilm. This slide contains two separate hopper chambers that are not interconnected.

foundly changed the flow rate at larger exit orifice sizes [20] as compared to the granular Beverloo flow law [7]. One recent experiment used repulsive magnetic particles in a quasi-2D hopper and reported clogging for small orifices, but did not systematically study clogging [21]. In that work, the particles repelled each other at moderate separations, and so it was not clear how the clogging related to the particle size (or even how to define that size). Another experiment studied the shapes of arches formed in 2D granular hoppers, finding that these shapes differed somewhat from simulated frictionless arches [22].

In this paper we experimentally study a quasi-two-dimensional emulsion as a model of a soft frictionless granular material. Our emulsion samples are oil droplets in water, stabilized by a surfactant [23]. The droplets are sandwiched between two parallel pieces of glass so that they are deformed into pancake-like disks. The droplets are in a hopper chamber, as shown in Fig. 1. In our experiments droplets only clog when the hopper opening is less than two diameters wide. Clogging arches involve only one or two droplets. Our results are a strong contrast

to prior results from two-dimensional experiments using hard frictional granular particles, which saw larger arches and which clog at larger opening sizes [6, 14, 16, 18, 24]. To vary the softness of the droplets, we conduct simulations using the Durian bubble model [25]. The simulation results show that the softness of the experimental droplets explains the ease of flow in the experiment. Our simulation results suggest that making the droplets harder (or reducing gravity) can potentially recover the previous experimental results for hard particles. This is a dramatic demonstration of the importance of softness to the clogging process, and shows that flowing particulate materials behave qualitatively different when the particles are easily deformable by the flow.

## II. METHODS

### A. Experiment

Our samples are oil-in-water emulsions prepared by a standard co-flow microfluidic technique [26]. In this technique, mineral oil (Fisher Scientific O121-1, density  $\rho_{\text{oil}} = 0.83 \text{ g/mL}$ ) is injected into a flowing stream of distilled water and surfactant. We use Fairy dishwashing detergent at mass fraction 0.025 as the surfactant, as has been done in previous work [23]. The microfluidic technique produces droplets of a desired size with  $\sim 3\%$  polydispersity. We control the size of the droplets by varying the flow rates of the oil and water in the microfluidic device. Typically we make droplets  $\sim 200 \mu\text{m}$  in diameter. In some cases we mix together two batches of droplets with different sizes, but for most of our results we study samples composed of a single batch of droplets. Sometimes the emulsion gets sheared when we add it to the sample chamber, resulting in a few droplets that are unusually small, or the coalescence of droplets so that some are unusually large. Examples of each can be seen in some of the images in this paper.

Each sample chamber is a sandwich of a spacer between two glass slides, as shown in Fig. 1(a). The spacer material is either transparent plastic film ( $\approx 120 \mu\text{m}$  thickness) or parafilm ( $\approx 130 \mu\text{m}$  thickness). For each of these, the spacer material is cut into a desired shape using scissors. We briefly put the parafilm chambers onto a hot plate to slightly melt the parafilm to seal the chamber. In each case, after the initial preparation, the sample chambers are additionally sealed with epoxy to prevent leakage or evaporation. As we use scissors and position the spacer materials onto the slides by hand, often the sample chambers are imperfect. However, given the simplicity and rapidity of making these chambers, we simply select the best sample chambers to use in our experiments, where the hopper exit is adequately shaped. Examples are shown in Figs. 2 and 4. The hopper angles are set to be  $32 - 35^\circ$ , close to To *et al.*'s experiment with an angle of  $34^\circ$  [18].

Should droplets flowing through the hopper clog, we

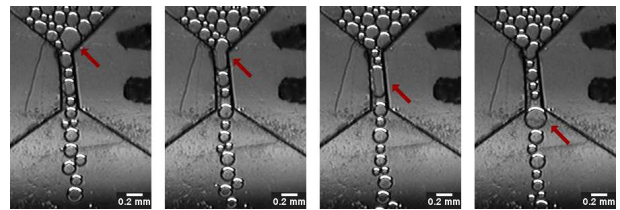


FIG. 2: This image sequence shows how a big droplet (marked with the arrow) can deform and squeeze through the hopper exit, if the surface tension is too low. The images are shown at 10 s time intervals.

need a way to unclog the system and get all of the droplets back to the entrance side of the hopper. We design our sample chambers with a side channel as shown in Fig. 1(b). This allows the sample chamber to be tilted and gives a path to move droplets from one side of the hopper to the other. The “C” shape on the left side of the individual chambers shown in Fig. 1(b) is to collect and hold any air bubble that might be present after the emulsion is added to the chamber.

Given the fairly large size of the droplets, we use a CCD camera and a macro-zoom lens to view our experiments, back-lighting the sample chamber. Jammed hoppers can also be seen by eye, which makes it possible to collect statistics without the camera. Video microscopy is used to count the number of droplets within a sample chamber, and to get an accurate measurement of the hopper angle of each chamber.

### B. Physics of flowing emulsions

While we are motivated by experiments on granular hopper flows, as described in Sec. I, there are several differences in our experiment. These differences are described in this section.

A superficial difference is that the density of the mineral oil droplets ( $\rho = 0.84 \text{ g/mL}$ ) is smaller than water ( $\rho = 1.00 \text{ g/mL}$ ), so our droplets float upward due to gravity. To make easier conceptual comparison with granular hoppers, we rotate all of our photographs so that the droplets are moving downward, for example Fig. 2.

A second difference is that our droplets are soft and deformable. The original work by To *et al.* used steel disks [15, 18, 27, 28], some authors use solid spheres [3, 16, 17, 22], and others use slightly deformable photoelastic disks [14, 24]. Our droplets are significantly more deformable. In the absence of external forces, a droplet would be spherical due to surface tension. However, in our experiment, droplets could potentially decrease their gravitational potential energy by deforming to squeeze through the hopper. This is indeed what happens if the surface tension is too small, or if the droplets are too large: an example is seen in Fig. 2. As the gravitational energy over a length scale  $d$  scales with droplet diameter as  $d^4$  while surface energy scales as  $d^2$ , larger droplets

will prefer to deform to reduce their gravitational energy [29]. Accordingly, to study clogging in our hoppers, we use a low amount of surfactant to keep the surface tension high, and also we use smaller droplets. This prevents the problem seen in Fig. 2. Were we to use large droplets, they would still clog if the hopper opening was sufficiently narrow, but this would then be entirely a surface tension effect rather than a study of clogging.

A third difference between our experiments and the prior granular experiments is that our oil droplets move through a viscous background fluid (water, viscosity  $\eta \approx 1$  mPa·s). The mineral oil droplets are themselves viscous ( $\eta \approx 20$  mPa·s) and experience viscous drag with the glass slides. The droplets contact the glass slides with a contact angle of  $19^\circ$  [23]; in other words, there is no lubricating water layer between the droplets and glass. The viscous drag on the droplets means that they move slowly, about  $0.20 - 0.25$  droplet diameters  $d$  per s depending on the conditions. This is in contrast to the granular experiments where particles spill out of the hopper quite rapidly [24]. This in principal might make clogging easier, as droplets moving toward the hopper exit have less inertia. Of course, the prior 2D granular experiments have some viscous drag from air, and also experience some sliding friction against their confining walls [16, 18].

A fourth difference is that in a granular container, the pressure is independent of depth (apart from near the free surface at the top, and at the bottom near the exit). This is known as the Janssen effect [30], and is due to the frictional forces acting on the particles from the container sidewalls [8, 31]. Due to our droplets not having static friction, we would not expect the Janssen effect to be present in our experiment. (Of course, some weight of the droplet pile is supported by the sloped hopper walls.) The lack of a Janssen effect was confirmed by an earlier experiment by our group, which found the internal pressure within a similar quasi-2D emulsion pile depended on depth in a tall container [23]. This also is similar to a granular hopper experiment using submerged particles [11] which did not find a Janssen effect. Accordingly, we might expect that clogging should be reduced in our experiment if large numbers of droplets exert forces on the droplets at the exit. On the other hand, the density mismatch between the oil and water is only  $\Delta\rho = 0.12$  g/mL, so the gravitational forces acting on our droplets are small albeit necessary for driving the hopper flow.

To be clear, the Janssen effect is thought to be irrelevant for understanding hopper flow. For example, one experiment removed the influence of gravity and provided strong evidence the Janssen effect is unrelated to clogging and flow rates through hoppers [10]. It is well known that granular hopper flow is independent of the amount of material in the hopper, as long as the amount of material is above some minimal threshold [7, 10, 17]. In contrast, that should not be the case in our experiments (and is confirmed by simulations that are discussed in the fol-

lowing subsection). As the weight above the droplets at the exit decreases, the probability of clogging increases. In other words, our experiment cannot be treated as in steady state, in contrast to granular hoppers [4, 17]. For granular experiments, this allows one to focus on the amount of material between clogs, using some method of unjamming a clog [17, 22]. In contrast, our experimental protocol is based on To *et al.* where we study the probability for the hopper to completely drain for a fixed initial number of droplets [18, 27].

### C. Simulations

Due to challenges in experimentally varying parameters such as surface tension or gravity over a wide range, we also simulate the hopper flow of emulsions. This is done with the Durian “bubble model” [25], using the version presented in Ref. [32] that allows each particle to have a variable number of nearest neighbors. While the model was designed for bubbles in flowing foams, it also works for emulsion droplets. Each droplet feels several forces. First is a repulsive contact force acting on droplet  $i$  from each neighboring droplet  $j$ , modeled as

$$\vec{F}_{ij}^{\text{contact}} = F_0 \left[ \frac{1}{|\vec{r}_i - \vec{r}_j|} - \frac{1}{|R_i + R_j|} \right] \vec{r}_{ij}, \quad (1)$$

using the droplet radii  $R_i$ , their positions  $\vec{r}_i$ , and the vector  $\vec{r}_{ij} = \vec{r}_j - \vec{r}_i$ . The neighbors  $j$  are defined as those droplets for which  $|\vec{r}_{ij}| < R_i + R_j$ .  $F_0$  acts like a spring constant and conceptually is due to the surface tension. In this model, rather than trying to deal with the droplet surface energy directly via describing the deformed droplet surface, droplets are treated as undeformed circles which repel each other only when they overlap. Neighboring droplets also exert viscous forces on each other if they move at different velocities,

$$\vec{F}_{ij}^{\text{viscous}} = b(\vec{v}_i - \vec{v}_j). \quad (2)$$

To model our experiment, we add three additional forces. First, we add in a repulsive force from the hopper walls similar to Eqn. 1,

$$\vec{F}_i^{\text{wall}} = F_0 \left[ \frac{1}{|\vec{r}_i - \vec{r}_{\text{wall}}|} - \frac{1}{R_i} \right] \hat{r}_{i,\text{wall}}, \quad (3)$$

where  $\vec{r}_{\text{wall}}$  is placed at the closest point on a wall to the droplet, and  $\hat{r}_{i,\text{wall}}$  is a unit vector pointing normal to the wall. Similar to the droplet-droplet contact forces,  $\vec{F}_i^{\text{wall}}$  only acts if a droplet overlaps with the wall, that is, if it is within a distance  $R_i$  to the wall. Second, we add in a gravitational force proportional to the mass of each droplet,

$$\vec{F}_i^{\text{gravity}} = -gR_i^2 \hat{y} \quad (4)$$

which points in the  $-\hat{y}$  direction. Third, we add in a viscous force between the droplets and the confining plates,

$$\vec{F}_{ij}^{\text{plates}} = -cR_i^2 \vec{v}_i, \quad (5)$$

which enforces a terminal velocity (equal to  $g/c$ ) for freely falling isolated droplets. Finally, following the original bubble model method [25, 32], we note that we are modelling a regime where inertia plays no role, and therefore these forces sum to zero for each droplet  $i$ :

$$\sum_j [\vec{F}_{ij}^{\text{contact}} + \vec{F}_{ij}^{\text{viscous}}] + \vec{F}_i^{\text{wall}} + \vec{F}_i^{\text{gravity}} - \vec{F}_i^{\text{plates}} = 0. \quad (6)$$

This can be rewritten as an equation for each droplet's velocity  $\vec{v}_i$  in terms of the positions and velocities of all the droplets [32]. This first order differential equation is integrated using the standard Runge-Kutta algorithm.

We simplify our simulations by setting  $b = c = 1$ . In practice, the viscous forces in the simulations are typically quite small, as the droplets flow slowly out of the hopper, and droplets generally move in similar directions to their neighbors ( $\vec{v}_i \approx \vec{v}_j$ ). The key control parameter thus is the ratio  $g/F_0$ , which expresses the relative importance of gravity to the contact forces between droplets. We set  $F_0 = 1$  for our simulations unless otherwise noted, and vary  $g$ . The velocities change very slowly, so rather than solving Eqn. 6 for all velocities simultaneously, we use the previous timestep's velocity values in Eqn. 2 for the neighbor velocities. Again, in practice,  $\vec{F}_i^{\text{viscous}}$  is small compared to the other forces, so this is a reasonable simplification. For the simulations, the hopper angle is  $\theta = 34^\circ$ , and we simulate 800 droplets with a Gaussian radius distribution with mean  $\langle R \rangle = 1$  and standard deviation  $\sigma_R = 0.1$ . A clog is defined to have occurred in the simulation when the maximum speed of all droplets is below  $10^{-10}g/c$ ,

We initialize the simulations by placing droplets in random positions above the hopper and with gravity in the opposite direction. The droplets then move until they have reached positions that minimize contact forces. At that point, gravity is reversed so that the droplets fall toward the hopper exit, much like the way the experiments are conducted. The resulting pile of droplets above the hopper exit resembles the experimental conditions.

### III. RESULTS

#### A. Experiment

To determine clogging probabilities, we load our sample chamber with 750 - 950 droplets. We then let these droplets flow through the sample chamber and observe if a clog forms. We repeat this 50 times for each sample chamber to measure the clogging probability  $P_{\text{clog}}$ . Figure 3(a) shows  $P_{\text{clog}}$  as a function of the hopper exit width  $w$  (normalized by the mean droplet diameter  $d$ ). The most striking result is that the widths at which clogging occurs are quite small. At  $w/d \approx 1.4$ , the droplets clog half of the experiments, and for larger hoppers, clogging is never observed. This is in stark contrast to the case of hard frictional particles, which clog half of the

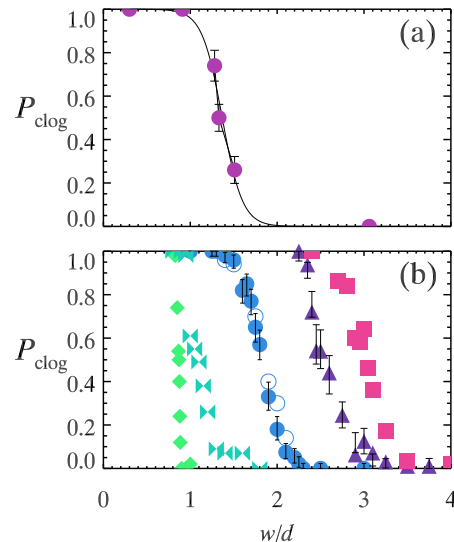


FIG. 3: The probability of clogging as a function of  $w/d$ , the ratio of the hopper exit width  $w$  to the droplet diameter  $d$ . (a) Experimental data corresponding to Table I. The solid line is a fit to the sigmoidal function  $P = [1 + \exp((w/d - a)/b)]^{-1}$  with  $P = 1/2$  at  $w/d = a = 1.37$  and width  $b = 0.17$ . The error bars are the uncertainty due to the finite number of trials ( $n = 50$ ) for a Poisson process. (b) Simulation data. For these data,  $F_0 = 1$ , and the gravity increases from left to right:  $g/F_0 = 10^{-1}, 3 \cdot 10^{-2}, 10^{-3}, 10^{-4}$ . The exception is the open circles, for which  $F_0 = 10$  and  $g/F_0 = 10^{-2}$ . Typical error bars are shown for some of the data, based on the finite number of trials ( $n = 100$  for the simulations).

$w/d$	$d$	$N$	$\theta$	$P_{\text{clog}}$
0.30	237 $\mu\text{m}$	867	32°	1.00
0.91	202 $\mu\text{m}$	947	35°	1.00
1.28	250 $\mu\text{m}$	771	33°	0.74
1.33	280 $\mu\text{m}$	786	35°	0.50
1.51	285 $\mu\text{m}$	764	33°	0.26
3.06	280 $\mu\text{m}$	923	34°	0.00

TABLE I: Details of the six experiments that measured clogging probabilities.  $w$  is the hopper exit width,  $d$  the mean droplet diameter,  $N$  is the number of droplets,  $\theta$  is the hopper angle, and  $P_{\text{clog}}$  is the probability of clogging based on 50 trials. The uncertainty of  $d$  is  $\pm 5 \mu\text{m}$ , and the uncertainty of  $w/d$  is  $\pm 0.03$ .

time at  $w/d \approx 4$  [18].

Note a caveat: the probability of clogging should be approximately constant for a given number of droplets flowing through the exit [15, 16, 24, 33]. With more droplets, there is more chance of observing clogging, if the probability of clogging per droplet is nonzero. We cannot perfectly control the number of droplets in our sample chamber, so the cases with more droplets will have  $P_{\text{clog}}$  larger. For the three points with  $0 < P_{\text{clog}} < 1$ , the number of droplets is fairly similar (see Table I). In



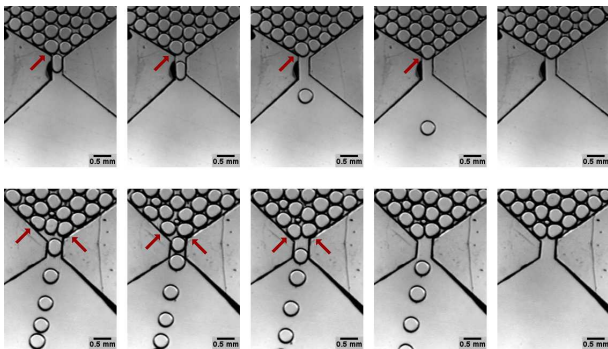


FIG. 4: These images show two examples of clogging. The top row shows a situation where one droplet clogs at the hopper exit ( $w/d = 0.81$ ). The bottom row shows a situation where two droplets form a small arch at the hopper exit ( $w/d = 1.00$ ). The arrows indicate the droplet(s) that will clog the opening. For the top row, the images are each 10 s apart, except for the final image which is 50 s later. For the bottom row, the images are each 5 s apart, except for the final image which is 30 s later.

the first experiment reported by To *et al.* they used 200 particles [18], approximately a quarter of the number we use. Their later work showed that with more particles  $P_{\text{clog}}$  moves to larger  $w/d$  [27]. They found  $P_{\text{clog}} = 1/2$  at  $w/d \approx 4.0$  for 200 particles, and  $\approx 4.8$  for 700 particles. Janda *et al.* found qualitatively similar results in their 2D granular experiment, with  $P_{\text{clog}} = 1/2$  increasing from  $w/d \approx 3$  with 50 particles to  $w/d \approx 5.5$  with 50000 particles [16]. Fitting our data to a sigmoidal function as shown in Fig. 3(a), we have a width  $\approx 0.2$ , slightly smaller than their widths  $\approx 0.3$  [18]. It is not clear that the sigmoidal fit we use is correct; To *et al.* used a different fit, and their data with gear-shaped particles had a decidedly non-sigmoidal shoulder [18]. Likewise Janda *et al.* used a different fit [16]. Our sparse data are not sufficient to distinguish subtle differences in these fits, so we stick with the simple sigmoidal fit.

Figure 4 shows two examples of clogged samples. The top case shows  $w/d \approx 0.8$  and a situation where the influence of surface tension is weak enough that one droplet can deform and slip through. However, after that first droplet, the remainder clog. The bottom case shows a small “arch” of two particles that clog at  $w/d \approx 1.0$ .

## B. Simulation

We find that in our system of soft frictionless droplets, that the probability of clogging in hopper flow is greatly reduced from prior published experiments that studied hard frictional particles [16, 18, 27]. In our experiment, we only see clogging with exit apertures significantly smaller than previously seen with frictional particles [5–9, 11]. We cannot separate the roles of softness and lack of friction for our particles.

To better understand this, we conduct simulations as

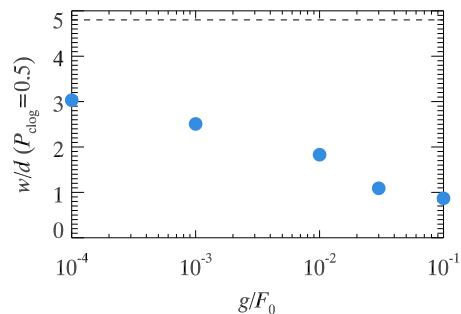


FIG. 5: A plot of the size of the hopper opening  $w/d$  for which  $P_{\text{clog}} = 1/2$  as a function of  $g/F_0$ . For lower values of gravity  $g$  (or equivalently, stiffer particles with larger  $F_0$ ), the data begin to approach the limiting value measured for hard steel disks,  $w/d = 4.8$  from Ref. [27].

described in Sec. II C. The simulations do not have friction, but they allow us to vary the relative importance of gravity and contact forces through the ratio  $g/F_0$ . As with the experiments, for each simulation we initialize the droplets in random positions above the hopper, let them fall, and observe if they completely flow out of the hopper or if they clog. Typically we do  $n = 100$  runs for each condition to measure  $P_{\text{clog}}$ .

For a moderate value  $g/F_0 = 10^{-2}$ , the simulation clogging probability curve looks qualitatively similar to the experiment [circles in Fig. 3(b)]. Varying  $g/F_0$  significantly shifts the clogging probability curve in Fig. 3(b), from  $g/F_0 = 10^{-1}$  (diamonds) to  $g/F_0 = 10^{-4}$  (squares). From these data, we extract the hopper opening width  $w/d$  for which  $P_{\text{clog}} = 0.5$  and plot this as a function of  $g/F_0$  in Fig. 5. As the importance of gravity is decreased, the data begin to approach the value measured in the experiments of To *et al.* that used steel disks (horizontal dashed line in Fig. 5) [18]. For gear-shaped particles, they found a slightly larger value,  $w/d = 4.0$  for  $P_{\text{clog}} = 0.5$  as compared to  $w/d = 3.6$  for the smooth disks (using 200 disks) [18]. Our results in Fig. 5 suggest that the relative influences of gravity and particle stiffness, quantified in the simulation by the ratio  $g/F_0$ , plays a more significant role for soft particles than the enhanced friction played in the prior experiments.

Figure 6 shows examples of arches found in the simulations. For the largest value of gravity, clogging is most typically due to one large droplet that reaches the exit when most other droplets have already exited [Fig. 6(a)]. This is equivalent to a droplet such as the large one shown in Fig. 2, but with fewer droplets above it and the driving pressure is not large enough to cause the large droplet to deform. Thus, the clogging probability curve for such a large value of  $g/F_0$  [green diamonds in Fig. 3(b)] has little to do with arch formation and more to do with the likelihood of an unusually large droplet being one of the last ones left in the hopper.

The more interesting cases are seen in Fig. 6(b-d) for lower values of  $g/F_0$ , corresponding to weaker gravity (or

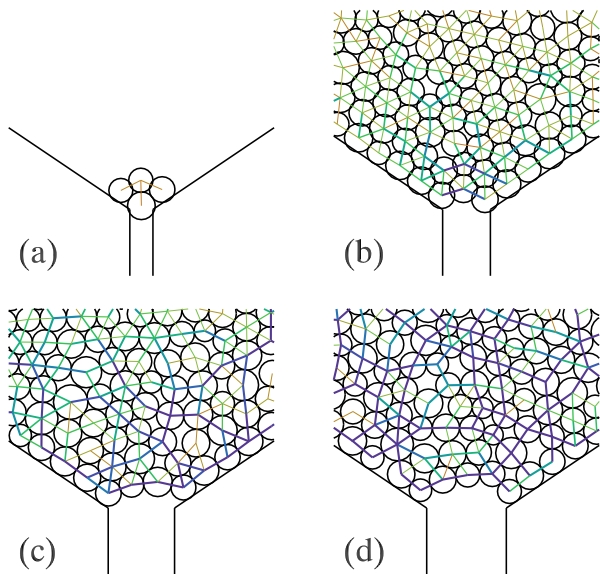


FIG. 6: Examples of arches found in the simulation. The parameter values are (a)  $g/F_0 = 10^{-1}$ ,  $w/d = 1.74$ ; (b)  $g/F_0 = 10^{-2}$ ,  $w/d = 3.6$ ; (c)  $g/F_0 = 10^{-3}$ ,  $w/d = 5.0$ ; (d)  $g/F_0 = 10^{-4}$ ,  $w/d = 6.04$ . The colored lines indicate contact forces between the droplets, relative to the gravitational force acting on an isolated droplet of the mean size. The thickest (purple) lines correspond to forces 8 or more times larger than the reference force. The numbers of droplets left in the hopper are (a) 4, (b) 190, (c) 400, and (d) 708. With more droplets present as in (d), the forces are larger as the arch supports more weight.

equivalently, stiffer droplets). It is apparent that large arches can form (up to 5 droplets) without requiring friction to be present. This is perhaps an unsurprising result, as the theory of To *et al.* that explains their data does not require friction [18].

#### IV. DISCUSSION

In our experiments, our droplets cannot sustain long arches, and clogging requires small openings. One possible explanation is the lack of static friction in our experiment; our result of reduced clogging qualitatively matches the trend seen by To *et al.* who found a lower clogging probability for smooth-surface disks compared to gear-shaped disks [18]. However, our simulation results show that even frictionless droplets can form large arches under certain conditions (Fig. 6). The key requirement is that the gravitational force must be small in comparison to the stiffness of the droplets. To rephrase this in physical terms, for an emulsion the surface tension must be high, or gravity must be weak, to be able to form large arches that can clog the hopper. In our experiment, despite the reduced influence of gravity (due to buoyancy

of the droplets) and their slower motion (due to viscous forces), gravity essentially breaks large arches due to a mechanism similar to what is seen in Fig. 2, albeit with subtler droplet deformations.

Our results with reduced gravity are the opposite of those seen in prior work that found reducing gravity prevented clogging [3]. In that work, the conclusion was that reducing the load on the arches at the exit would allow vibrations or other noise to destroy the arch [3, 34]. That is, the weight of the grains above the exit applies a compatible load that strengthens the arch formed from hard granular materials. In contrast, our soft particles are deformed by this load and thus the load can strengthen the arch (at low loads) or break the arch (at high loads). More significantly, we have no source of incompatible forces that disrupt a stable arch once formed, unlike the prior work [3]. For smaller droplets for which Brownian motion might play a role, it is possible that decreasing gravity would decrease clogging, the opposite of our present results for non-Brownian droplets.

Our results also contrast with centrifuge experiments of Dorbolo *et al.*, which found that clogging was uninfluenced by gravity [35]. These experiments do not have added vibrations, so provide a complementary view to Ref. [3]. The difference between these experiments and our work is likely explainable by their use of glass and steel beads. For glass beads, estimating their modulus as  $E = 70$  GPa, density as  $\rho = 2.6$  g/cm<sup>3</sup>, and using their radius  $R = 200$   $\mu$ m, one can use the Hertzian contact model to estimate the deformation of a spherical particle due to the gravitational weight of the particles above. Assuming the imposed weight is approximately 10 times larger than the weight of an individual sphere, the deformation  $d$  of a glass bead under the maximum imposed gravity ( $20g$ ) would be approximately  $d/R = 10^{-5}$  for Ref. [35]. For our simulations under the same assumptions about the imposed weight, the expected deformation of droplets in the clogging arch is  $d/R \approx 40g/F_0$ , so  $4 \times 10^{-3}$  for our lowest value of  $g/F_0$  (defining  $d$  as the overlap between two droplets). As Fig. 5 suggests, we have not yet reached the hard particle limit yet in our simulations, so it is not surprising to think that the experiments of Ref. [35] are in a low-gravity limit where gravity is unimportant for clogging. This suggests that there are opportunities to explore clogging using softer granular particles where gravity should have an observable influence on clogging.

Overall, our results demonstrate that the flow of soft particles is qualitatively different from the case of hard particles. This potentially has implications for other situations where particles have soft long-range interactions such as magnetic particles [21], merging traffic [36], and perhaps flowing bacteria [37].

We thank D. Chen, K. Desmond, and D. Durian for helpful discussions. This work was supported by the National Science Foundation (CBET-1336401).

- 
- [1] H. M. Jaeger, S. R. Nagel, and R. P. Behringer, Granular solids, liquids, and gases, *Rev. Mod. Phys.*, **68**, 1259–1273 (1996).
- [2] Y. Forterre and O. Pouliquen, Flows of dense granular media, *Ann. Rev. Fluid Mech.*, **40**, 1–24 (2008).
- [3] I. Zuriguel, D. R. Parisi, R. C. Hidalgo, C. Lozano, A. Janda, P. A. Gago, J. P. Peralta, L. M. Ferrer, L. A. Pugnaloni, E. Clément, D. Maza, I. Pagonabarraga, and A. Garcimartín, Clogging transition of many-particle systems flowing through bottlenecks, *Scientific Reports*, **4**, 7324 (2014).
- [4] I. Zuriguel, Invited review: Clogging of granular materials in bottlenecks, *Papers in Physics*, **6**, 060014 (2014).
- [5] W. E. Deming and A. L. Mehring, The gravitational flow of fertilizers and other comminuted solids, *Ind. Eng. Chem.*, **21**, 661–665 (1929).
- [6] R. L. Brown and J. C. Richards, Two- and Three-Dimensional flow of grains through apertures, *Nature*, **182**, 600–601 (1958).
- [7] W. A. Beverloo, H. A. Leniger, and J. van de Velde, The flow of granular solids through orifices, *Chem. Eng. Sci.*, **15**, 260–269 (1961).
- [8] R. M. Nedderman, U. Tuzun, S. B. Savage, and G. T. Houlsby, The flow of granular materials—I : Discharge rates from hoppers, *Chem. Eng. Sci.*, **37**, 1597–1609 (1982).
- [9] H. Sheldon and D. Durian, Granular discharge and clogging for tilted hoppers, *Granular Matter*, **12**, 579–585 (2010).
- [10] M. A. Aguirre, J. G. Grande, A. Calvo, L. A. Pugnaloni, and J. C. Géminard, Pressure independence of granular flow through an aperture, *Phys. Rev. Lett.*, **104**, 238002 (2010).
- [11] T. J. Wilson, C. R. Pfeifer, N. Mesyngier, and D. J. Durian, Granular discharge rate for submerged hoppers, *Papers in Physics*, **6**, 060009 (2014).
- [12] R. T. Fowler and J. R. Glastonbury, The flow of granular solids through orifices, *Chem. Eng. Sci.*, **10**, 150–156 (1959).
- [13] D. C. Hong and J. A. McLennan, Molecular dynamics simulations of hard sphere granular particles, *Physica A*, **187**, 159–171 (1992).
- [14] F. Vivanco, S. Rica, and F. Melo, Dynamical arching in a two dimensional granular flow, *Granular Matter*, **14**, 563–576 (2012).
- [15] K. To, Jamming transition in two-dimensional hoppers and silos, *Phys. Rev. E*, **71**, 060301 (2005).
- [16] A. Janda, I. Zuriguel, A. Garcimartín, L. A. Pugnaloni, and D. Maza, Jamming and critical outlet size in the discharge of a two-dimensional silo, *Europhys. Lett.*, **84**, 44002 (2008).
- [17] C. C. Thomas and D. J. Durian, Fraction of clogging configurations sampled by granular hopper flow, *Phys. Rev. Lett.*, **114**, 178001 (2015).
- [18] K. To, P. Y. Lai, and H. K. Pak, Jamming of granular flow in a two-dimensional hopper, *Phys. Rev. Lett.*, **86**, 71–74 (2001).
- [19] F. C. Franklin and L. N. Johanson, Flow of granular material through a circular orifice, *Chem. Eng. Sci.*, **4**, 119–129 (1955).
- [20] Y. Bertho, C. Becco, and N. Vandewalle, Dense bubble flow in a silo: An unusual flow of a dispersed medium, *Phys. Rev. E*, **73**, 056309 (2006).
- [21] G. Lumay, J. Schöckmel, D. Henández-Enríquez, S. Dorbolo, N. Vandewalle, and F. Pacheco-Vázquez, Flow of magnetic repelling grains in a two-dimensional silo, *Papers in Physics*, **7**, 070013 (2015).
- [22] A. Garcimartín, I. Zuriguel, L. A. Pugnaloni, and A. Janda, Shape of jamming arches in two-dimensional deposits of granular materials, *Phys. Rev. E*, **82**, 031306 (2010).
- [23] K. W. Desmond, P. J. Young, D. Chen, and E. R. Weeks, Experimental study of forces between quasi-two-dimensional emulsion droplets near jamming, *Soft Matter*, **9**, 3424–3436 (2013).
- [24] J. Tang, S. Sagdiphour, and R. P. Behringer, Jamming and flow in 2D hoppers, *AIP Conf. Proc.*, **1145**, 515–518 (2009).
- [25] D. J. Durian, Foam mechanics at the bubble scale, *Phys. Rev. Lett.*, **75**, 4780–4783 (1995).
- [26] R. K. Shah, H. C. Shum, A. C. Rowat, D. Lee, J. J. Agresti, A. S. Utada, L.-Y. Chu, J.-W. Kim, A. Fernandez-Nieves, C. J. Martinez, and D. A. Weitz, Designer emulsions using microfluidics, *Materials Today*, **11**, 18–27 (2008).
- [27] K. To, P.-Y. Lai, and H. K. Pak, Flow and jam of granular particles in a two-dimensional hopper, *Physica A*, **315**, 174–180 (2002).
- [28] K. To and P.-Y. Lai, Jamming pattern in a two-dimensional hopper, *Phys. Rev. E*, **66**, 011308 (2002).
- [29] V. F. Weisskopf, Search for simplicity: Mountains, waterwaves, and leaky ceilings, *Am. J. Phys.*, **54**, 110–111 (1986).
- [30] H. A. Janssen, Versuche über Getreidedruck in Silozellen, *Zeitschr. d. Vereines deutscher Ingenieure*, **39**, 1045–1049 (1895).
- [31] J. H. Shaxby, J. C. Evans, and V. Jones, On the properties of powders. the variation of pressure with depth in columns of powders, *Trans. Faraday Soc.*, **19**, 60–72 (1923).
- [32] S. Tewari, D. Schiemann, D. J. Durian, C. M. Knobler, S. A. Langer, and A. J. Liu, Statistics of shear-induced rearrangements in a two-dimensional model foam, *Phys. Rev. E*, **60**, 4385–4396 (1999).
- [33] P. G. Lafond, M. W. Gilmer, C. A. Koh, E. D. Sloan, D. T. Wu, and A. K. Sum, Orifice jamming of fluid-driven granular flow, *Phys. Rev. E*, **87**, 042204 (2013).
- [34] M. E. Cates, J. P. Wittmer, J. P. Bouchaud, and P. Claudin, Jamming, force chains, and fragile matter, *Phys. Rev. Lett.*, **81**, 1841–1844 (1998).
- [35] S. Dorbolo, L. Maquet, M. Brandenbourger, F. Ludewig, G. Lumay, H. Caps, N. Vandewalle, S. Rondia, M. Mélard, J. van Loon, A. Dowson, and S. Vincent-Bonnieu, Influence of the gravity on the discharge of a silo, *Granular Matter*, **15**, 263–273 (2013).
- [36] D. Helbing, Traffic and related self-driven many-particle systems, *Rev. Mod. Phys.*, **73**, 1067–1141 (2001).
- [37] E. Altshuler, G. Mino, C. Perez-Penichet, L. D. Rio, A. Lindner, A. Rousselet, and E. Clément, Flow-controlled densification and anomalous dispersion of *E. coli* through a constriction, *Soft Matter*, **9**, 1864–1870 (2013).